

Does Reinforcement Learning Really Incentivize Reasoning Capacity in LLMs Beyond the Base Model?

Yang Yue^{1*†}, Zhiqi Chen^{1*}, Rui Lu¹, Andrew Zhao¹, Zhaokai Wang², Yang Yue¹, Shiji Song¹, and Gao Huang^{1✉}

¹LeapLab, Tsinghua University ²Shanghai Jiao Tong University

* Equal Contribution † Project Lead ✉ Corresponding Author

Reinforcement Learning with Verifiable Rewards (RLVR) has recently demonstrated notable success in enhancing the reasoning capabilities of large language models (LLMs), particularly in mathematics and programming tasks. It is widely believed that RLVR enables LLMs to continuously self-improve, thus acquiring novel reasoning abilities that exceed corresponding base models' capacity. In this study, however, we critically re-examines this assumption by measuring the pass@ k metric with large values of k to explore the reasoning capability boundary of the models across a wide range of model families, RL algorithms and math/coding benchmarks. Surprisingly, RLVR training does *not*, in fact, elicit fundamentally new reasoning patterns. We observed that while RL-trained models outperform their base models at smaller values of k (e.g., $k=1$), base models can achieve a comparable or even higher pass@ k score compared to their RL counterparts at large k values. Further analysis shows that the reasoning paths generated by RL-trained models are already included in the base models' sampling distribution, suggesting that most reasoning abilities manifested in RL-trained models are already obtained by base models. RL training boosts the performance by biasing the model's output distribution toward paths that are more likely to yield rewards, therefore sampling correct responses more efficiently. But this also limits their exploration capacity, resulting in a narrower reasoning capability boundary compared to base models. Similar results are observed in visual reasoning tasks trained with RLVR. Moreover, we find that, different from RLVR, distillation can genuinely introduce new knowledge into the model. These findings underscore a critical limitation of RLVR in advancing LLM reasoning abilities, which requires us to rethink the impact of RL training in reasoning LLMs and the need of a better training paradigm.

Project Page: <https://limit-of-RLVR.github.io>

1. Introduction

The development of reasoning-centric large language models (LLMs), such as OpenAI-o1 (Jaech et al., 2024), DeepSeek-R1 (Guo et al., 2025), and Kimi-1.5 (Team et al., 2025), has significantly advanced the frontier of LLM capabilities, particularly in solving complex logical tasks involving mathematics and programming. In contrast to traditional instruction-tuned approaches that rely on human-curated annotations (Achiam et al., 2023; Grattafiori et al., 2024), the key driver behind this leap forward is large-scale *Reinforcement Learning with Verifiable Rewards* (RLVR) (Lambert et al., 2024; Guo et al., 2025). RLVR starts with a pretrained base model or one fine-tuned on long chains of thought (CoT) data, optimizing it via reinforcement learning based on simple, automatically computable rewards.

Correspond to: {le-y22, zq-chen23}@mails.tsinghua.edu.cn, gaohuang@tsinghua.edu.cn.

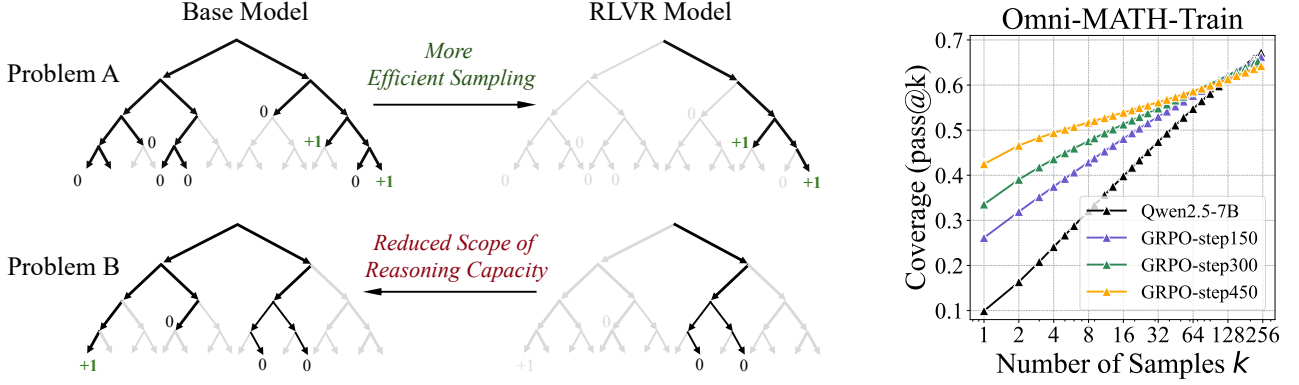


Figure 1: **(Left)** The effect of RLVR on LLM’s reasoning ability. Search trees are generated by repeated sampling from the base and RLVR-trained models for a given problem. Grey indicates paths that are unlikely to be sampled by the model, while **black** indicates paths that are likely to be sampled. **Green** indicates correct paths, which has positive rewards. Our key finding is that all reasoning paths in the RLVR model are already present in the base model. For certain problems like Problem A, RLVR training biases the distribution toward rewarded paths, improving sampling efficiency. However, this comes at the cost of reduced scope of reasoning capacity: For other problems like Problem B, the base model contains the correct path, whereas that of the RLVR model does not. **(Right)** As RLVR training progresses, the average performance (*i.e.*, pass@1) improves, but the coverage of solvable problems (*i.e.*, pass@256) decreases, indicating a reduction in the model’s reasoning upper bound.

These rewards are determined by whether the model’s output matches a ground-truth solution in mathematics or passes unit tests in code, thus enabling scalability without human labeling. This framework has gained significant attention due to its simplicity and practical effectiveness. It is widely believed that RLVR enables models to autonomously incentivize advanced reasoning behaviors, such as enumeration, self-reflection, and iterative refinement, which are not present in base models (Guo et al., 2025). Consequently, RLVR is viewed as a pathway to self-evolving LLMs with continuously expanding reasoning capabilities, potentially advancing us closer to stronger intelligence (Guo et al., 2025).

However, despite the empirical successes of RLVR, a critical question remains in the pursuit of continually self-evolving reasoning abilities:

Does RLVR really bring novel reasoning capabilities to LLMs? If so, what does the model learn from RLVR training?

In order to rigorously answer this question, we first need to determine the boundary of reasoning capability of base and RL-trained models. Traditional metrics use single-pass success rates or average nucleus sampling (Holtzman et al., 2019) to measure average-case performance. However, in our work, we highlight an important oversight behind such metrics: *a model’s true reasoning potential may be underestimated if it fails on difficult problems after only a few attempts, even if it could succeed with more sampling.* To address this, we employ a simple method, namely the pass@ k metric (Brown et al., 2024), where a problem is considered solved if any of the k samples is correct. The idea is simple: What if we invest heavily in sampling for the base model with an enormous k ? Can its performance match the RLVR-trained one? By giving the model a large number of trials to solve a problem, we are able to evaluate the boundary of reasoning capabilities of both base and RL-trained models. This provides a critical and rigorous test on whether the RLVR training yields fundamentally transcending capacity—enabling the model to solve problems that the base model cannot.

We conduct extensive experiments across diverse benchmarks, including mathematics, code generation, and visual reasoning, spanning multiple LLM families, model sizes, and RL algorithms. Using the pass@ k metric, we compare the performance of base models with their RL-trained counterparts. We find several perhaps surprising discoveries that may alter the conventional understanding of reasoning models and RLVR training, as follows:

- **RLVR-trained models perform worse than base models in pass@ k at large k values.** Although RL-trained models consistently outperform their base models in small k as shown in previous

work (Guo et al., 2025), it is highly surprising that base models consistently surpass RL-trained models across all benchmarks and LLM families as k increases. More notably, at sufficiently large k , base models achieve even higher pass@ k scores than their RL-enhanced counterparts. This means that the base model without any RL training can already generate the correct answers to problems that were previously considered only solvable for RL-trained models by aggressively sampling different approaches. We manually check the CoTs of these correct answers and find most of problems has *at least one* CoT to be correct. This suggests that RL training does *not* improve, but even downgrade, LLMs’ potential scope of reasoning capability.

- **RLVR boosts sampling efficiency but reduces the scope of reasoning capacity.** To further investigate this phenomenon, we conduct perplexity analysis. Our findings show that reasoning paths generated by RLVR-trained models already exist within the base models’ output distribution with considerable probability density, indicating that these reasoning patterns and CoTs are not totally strange and unachievable for base models. RLVR training contributes to reasoning by biasing the model toward rewarded reasoning paths, thereby increasing the likelihood of sampling correct reasoning paths. However, this efficiency gain also comes at a cost: RL training reduces the model’s exploration capacity, resulting in smaller coverage of solvable problems at large k (see Figure 1 right), suggesting its reduced scope of reasoning capacity. This challenges the common belief that RLVR elicits transcending reasoning ability. Instead, the reasoning capacity boundary of RLVR-trained models may be bounded by the capabilities of base model. The effect of RLVR on LLM’s reasoning ability is illustrated in Figure 1 left.

- **RLVR algorithms perform similarly and remain far from optimal.** Although different RL algorithms (*e.g.*, PPO, GRPO, Reinforce++) show slight variations in performance, it does not make essential difference. As shown in Figure 7 top, we define the difference between the RL model’s pass@1 and the base model’s pass@ k (*i.e.*, an potential performance upper-bound; we use $k = 256$) as the *sampling efficiency gap* (Δ_{SE}), which quantifies how effectively an RL algorithm approaches optimal sampling efficiency. We found that different RL algorithms produce only slight variations in Δ_{SE} , yet the gap remains consistently large across all methods. This suggests that current RL approaches, which primarily work by improve sampling efficiency, are still far from optimal.

- **RLVR and distillation are fundamentally different.** While RL improves sampling efficiency, distillation can genuinely introduce new knowledge into the model. As a result, distilled models often exhibit an expanded scope of reasoning capability beyond that of the base model by learning from distilled models, in contrast to RLVR-trained models whose capacity remains bounded by the base.

In conclusion, our results collectively indicate that RLVR, in its current form, is insufficient to incentivize transcending capabilities beyond the base model’s limits. Our work not only discovers findings that fundamentally challenge previous understanding on RLVR and its impact in reasoning models, but also implies that RLVR in itself might be inadequate to push forward the boundary of reasoning abilities.

2. Preliminaries

In this section, we first introduce the fundamentals of RLVR. We then provide a detailed explanation of pass@ k , the metric used to evaluate the reasoning boundary.

2.1. Reinforcement Learning with Verifiable Rewards

Verifiable Rewards. Let π_θ be an LLM with parameters θ that generates a token sequence $\mathbf{y} = (y_1, \dots, y_T)$ conditioned on a natural-language prompt x . A deterministic *verifier* \mathcal{V} returns a binary reward: $r = \mathcal{V}(x, \mathbf{y}) \in \{0, 1\}$, where $r = 1$ if and only if the model’s final answer is exactly correct (*e.g.*, the numeric result matches the ground truth in math, or all unit tests pass in code). A format reward may also be added to encourage the model to explicitly separate the reasoning process from the final answer. The goal of RL is to learn a policy to maximize the expected reward: $J(\theta) = \mathbb{E}_{x \sim \mathcal{D}} [\mathbb{E}_{\mathbf{y} \sim \pi_\theta(\cdot|x)}[r]]$, where \mathcal{D} is the distribution of prompts.

RLVR algorithms. Proximal Policy Optimization (PPO) (Schulman et al., 2017) proposed using the

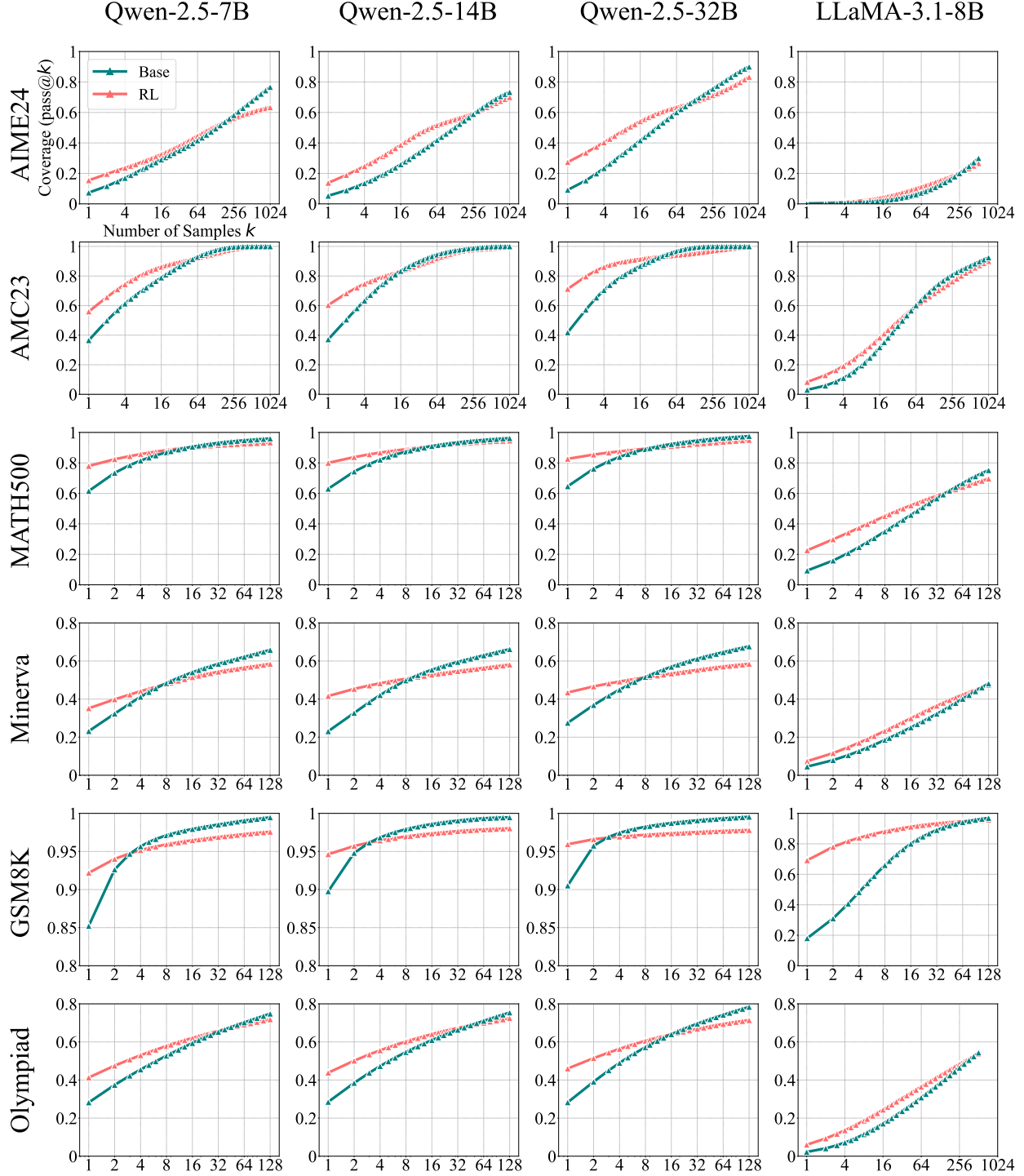


Figure 2: Pass@ k curves of base models and their zero-RL-trained counterparts across multiple mathematical benchmarks. When k is small, RL-trained models outperform their base versions. However, as k increases to the tens or hundreds, base models consistently catch up with RL-trained models across all benchmarks and LLM families without exception. Eventually, base models surpass RL-trained models.

following clipped surrogate to maximize the objective:

$$\mathcal{L}_{\text{CLIP}} = \mathbb{E} [\min(r_t(\theta)A_t, \text{clip}(r_t(\theta), 1 - \epsilon, 1 + \epsilon)A_t)], \quad (1)$$

where $r_t(\theta) = \pi_\theta(y_t|x, \mathbf{y}_{<t})/\pi_{\theta_{\text{old}}}(y_t|x, \mathbf{y}_{<t})$, and A_t is the advantage estimated by a value network V_ϕ . A KL divergence term is also applied, either as a reward penalty or directly in the loss function, to

constrain the model from deviating too far from the original policy.

To reduce memory and computational overhead, several critic-free variants have been proposed. GRPO (Shao et al., 2024) estimate the advantage with a normalized reward within a group of responses to the same question: $A_i = [r_i - \text{mean}(\mathbf{r})]/\text{std}(\mathbf{r})$, where $\mathbf{r} = \{r_1, \dots, r_G\}$ denotes the set of rewards for a group of G sampled responses. RLOO (Ahmadian et al., 2024) instead adopts a leave-one-out baseline within each batch \mathcal{B} . Its advantage is defined as $A_i = r_i - \frac{1}{|\mathcal{B}|-1} \sum_{j \neq i} r_j$.

Policy Gradient. PPO and its variants belong to the policy gradient class of reinforcement learning (Williams, 1992; Sutton et al., 1998). These methods learn exclusively from *on-policy samples*, i.e., samples generated by the current LLM. In the context of verifiable binary rewards, the training objective is equivalent to *maximizing the log-likelihood of samples with correct answers and minimizing the likelihood of those with incorrect answers*.

Zero RL Training applies reinforcement learning directly to the base model without any supervised fine-tuning (SFT) on long CoT reasoning data (Guo et al., 2025). To clearly study the effect of RLVR, we follow this zero-RL setting for all math tasks using open-source base models. However, for coding and visual reasoning tasks, no previous open-source work adopts a strict zero-RL setting, mainly due to training instability and limited effectiveness. Instead, these tasks typically use instruction-tuned models as starting points. We follow this convention, which is reasonable for studying the effect of RL on reasoning ability, as these models are primarily fine-tuned on general instruction-following data rather than long-form CoT reasoning data.

2.2. Metrics for LLM Reasoning Capacity Boundary

Accurately measuring the reasoning ability boundary of base and RL models is challenging, as methods like single-pass greedy decoding or the average of a few rounds of nucleus sampling (Holtzman et al., 2019) reflect average-case performance rather than the model’s upper bound. For example, consider a traditional avg@8 approach, where 8 responses are sampled for an extremely difficult problem. If none of the responses are correct, the value is 0/8. However, after more trials such as 128, the model may solve the problem, indicating that the reasoning boundary can eventually overcome this challenge.

To accurately measure the reasoning ability boundaries of LLMs, we extend the commonly used pass@ k metric from code generation (Chen et al., 2021) to all tasks with verifiable rewards. Given a problem, we sample k outputs from the model. The pass@ k value for this question is 1 if at least one of the k samples passes verification; otherwise, it is 0. The average pass@ k value over the dataset reflects the proportion of problems in the dataset that the model can solve within k trials, providing a rigorous evaluation of the reasoning capacity coverage of LLMs.

Directly computing pass@ k using only k sampled outputs per problem can lead to high variance. To mitigate this, we follow the unbiased estimation method proposed by Chen et al. (2021). Specifically, for each problem x_i from the evaluation dataset \mathcal{D} , we generate n samples ($n \geq k$) and count the number of correct samples as c_i . The unbiased estimator of pass@ k over the dataset is given by:

$$\text{pass@}k := \mathbb{E}_{x_i \sim \mathcal{D}} \left[1 - \frac{\binom{n-c_i}{k}}{\binom{n}{k}} \right] \quad (2)$$

With this formulation, we can easily estimate pass@ k with low variance across all $k \leq n$.

For coding tasks, where a compiler and predefined unit test cases are used as verifiers, the pass@ k value can accurately reflect whether the model can solve the problem. However, the issue of “hacking” can become pronounced in mathematics as k increases. In math problems, a model may generate an incorrect chain of thought but still accidentally arrive at the correct answer in one of many samplings, a scenario that is often overlooked by previous metrics. To address this, we filter out problems that are easily “hacked” and then manually check the correctness of CoT for a subset of model outputs. By combining these measures, we rigorously evaluate the limit of LLM’s reasoning capacity as detailed in Section 3.1.

Table 1: Experimental setup for assessing RLVR’s effect on the reasoning boundaries of LLMs across different tasks.

Task	Start Model	RL Framework	RL Algorithm(s)	Benchmark(s)
Mathematics	LLaMA-3.1-8B	SimpleRLZoo Oat-Zero	GRPO	GSM8K, MATH500 Minerva, Olympiad AIME24, AMC23
	Qwen-2.5-7B/14B/32B-Base Qwen-2.5-Math-7B			
Code Generation	Qwen-2.5-7B-Instruct	Code-R1	GRPO	LiveCodeBench HumanEval+
Visual Reasoning	Qwen-2.5-VL-7B	EasyR1	GRPO	MathVista MathVision
Deep Analysis	Qwen-2.5-7B-Base	VeRL	PPO, GRPO Reinforce++ RLOO, ReMax, DAPO	Omni-Math-Rule MATH500
	Qwen-2.5-7B-Instruct DeepSeek-R1-Distill-Qwen-7B			

3. RLVR’s Effect on Reasoning Capacity Boundary

With the evaluation metrics for reasoning boundaries established, we now conduct a comprehensive evaluation of the base and RLVR models through extensive experiments. Our analysis is organized by task category, covering three representative domains: mathematics, code generation, and visual reasoning. The overall experimental setup is summarized in Table 1.

Evaluation Protocol. For all sampling procedures involving both base and RL-trained models, we use a temperature of 0.6 and a top- p value of 0.95, allowing a maximum generation of 16,384 tokens. We also show the effect of different temperature settings in Figure 10. For evaluation of the base model, a common practice is to include few-shot examples in the prompt to guide both the output formatting and the reasoning process (Grattafiori et al., 2024; Yang et al., 2024; Liu et al., 2024). However, to ensure a fair and unbiased comparison, we deliberately avoid using few-shot prompts for base models, eliminating any potential confounding effects on reasoning that might be introduced by in-context examples. For evaluating both the base and RLVR models, we use the same zero-shot prompt as in RLVR training, or the default prompt provided by the benchmark, ensuring a consistent setup across both models. Interestingly, although base models often produce unformatted or non-sensical responses without few-shot guidance, we observe that with sufficient sampling, they are still capable of generating correctly formatted outputs and successfully solving complex problems. Prompt templates for training and evaluation are provided in Appendix B.

3.1. RLVR for Mathematical Reasoning

Models and Benchmarks. In math problems, models are required to generate a reasoning process (*i.e.*, CoT) along with the final answer. To ensure the robustness of our conclusions, we experiment with multiple LLM families, primarily Qwen-2.5 (7B/14B/32B base variants) (Yang et al., 2024) and additionally LLaMA-3.1-8B (Grattafiori et al., 2024). We adopt RLVR-trained models released by SimpleRLZoo (Zeng et al., 2025), which train zero-RL models using GRPO on GSM8K and the MATH training set, with correctness reward only, excluding any format-based reward. We compare the pass@ k curves of base and zero-RL models on benchmarks of varying difficulty: GSM8K (Cobbe et al., 2021), MATH500 (Hendrycks et al., 2021), Minerva (Lewkowycz et al., 2022), Olympiad (He et al., 2024), AIME24, and AMC23. Additionally, we include the RL model Oat-Zero-7B, based on Qwen-2.5-7B-Base and trained using the Oat-Zero framework, for further comparison (Liu et al., 2025b). This model is characterized by strong performance on the challenging AIME24 benchmark, achieving an average of 43.4% points, substantially higher than the base model’s performance of below 10%.

The Effect of RLVR: Increased Likelihood of Correct Samples, Decreased Coverage of Solvable Problems. As shown in Figure 2, we consistently observe a contrasting trend between small and large k values. When k is small (*e.g.*, $k = 1$, equivalent to average-case accuracy), RL-trained models outperform their base counterparts. This aligns with the common observation that RL improves performance, suggesting that RLVR makes models significantly more likely to sample correct responses. However, as k increases to the tens or hundreds, base models consistently catch up with RL-trained

models across all benchmarks and LLM families without exception. Notably, the $\text{pass}@k$ curves of base models exhibit a steeper upward trend compared to their RL-trained versions. Ultimately, the base model surpasses the RL-trained model at sufficiently large k , indicating that the coverage of solvable problems by the base model is broader than that of the RL-enhanced version. For example, on the Minerva benchmark with a 32B-sized model, the base model outperforms the RL-trained model by approximately 9% at $k = 128$, implying that it can solve around 9% more problems in the validation set.

We further examine RL models trained with Oat-Zero. As shown in Figure 3, although the RL model initially demonstrates a strong performance, nearly 30% higher than the base model, it is eventually surpassed by the base model. Based on these results, we conclude that RLVR increases the likelihood of sampling correct responses at low k , but narrows the model’s overall coverage. We further analyze the root cause of this phenomenon in Section 4.1.

CoT Case Analysis. We present the sampled correct CoTs from the base model in Figure 18 and Figure 19, manually selected from 2048 samplings for the hardest questions in AIME24. The responses from the base model tend to be long CoTs and exhibit reflective behavior, highlighting the strong reasoning ability inherent in the base model.

Validity of Chain-of-Thought. For mathematical problems, the common evaluation is based solely on the correctness of the final answer, without considering the validity of the intermediate CoT. However, as k increases, the risk of “hacking” may become more pronounced when a model accidentally arrives at the correct answer through an incorrect CoT. To accurately reflect the reasoning ability boundary using $\text{pass}@k$, it is important to assess how many of the solved problems result from sampling genuinely correct CoTs, rather than from lucky guesses.

Following (Brown et al., 2024), we manually inspect all CoTs that led to correct answers on the most challenging solvable problems in the GSM8k dataset—those with an average accuracy below 5% but above 0%. The base model answered 25 such questions, with 24 containing *at least one* correct CoT. Similarly, the RL-trained model answered 25 questions, 23 of which included *at least one* correct CoT. These results suggest that even on the hardest questions in GSM8k, problem-solving primarily results from sampling valid reasoning paths rather than relying on lucky guesses, implying that $\text{pass}@k$ at large k values can serve as a relatively accurate indicator of a model’s reasoning boundary.

We also manually check the CoTs for the most challenging AIME24 benchmark. To begin, we introduce a filtering mechanism designed to eliminate easily guessable problems. Specifically, we prompt Qwen-7B-Base to answer questions directly, without using chain-of-thought reasoning, and sample answers multiple times. If a problem can be answered correctly with a low but non-zero probability (e.g., $<5\%$), we consider it guessable and remove it. Problems that can be directly answered correctly with a high probability are retained, as they are likely easier and solvable using valid CoTs. The base and RL model $\text{pass}@k$ curves on this filtered AIME24 can be found in Figure 9, showing similar trending with previous results. While this filtering method is heuristic, it proves effective. Applying it to AIME24 (30 questions) results in a subset of 18 questions. We then prompt the models to answer these filtered questions using CoT reasoning. Then we perform a manual inspection of all CoTs that led to correct answers on the hardest problems—those with an average accuracy below 5%. The base model answered 7 such questions, with 5 out of 6 containing *at least one* correct CoT (excluding one ambiguous case of correctness due to skipped reasoning steps.). Similarly, the RL-trained model answered 6 questions, 4 of which included *at least one* correct CoT. These results suggest that, even for the hardest questions in the challenging AIME24, base model can sampling valid reasoning paths to solve the problems.

3.2. RLVR for Code Generation

Models and Benchmarks. We adopt the open-source Code-R1 (Liu & Zhang, 2025) and evaluate its RLVR-trained model, CodeR1-Zero-Qwen2.5-7B, which trains zero-RL models on 12K LeetCode

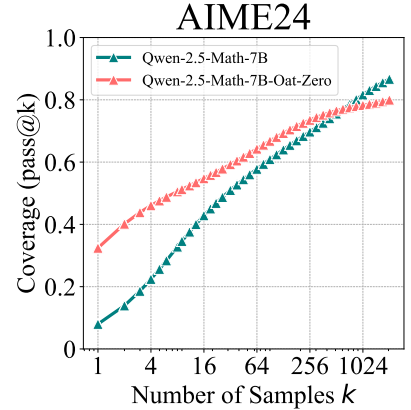


Figure 3: Oat-Zero for AIME24.

and TACO samples over 832 steps, based on Qwen2.5-7B-Instruct-1M (Yang et al., 2025). A binary correctness reward is provided by the compiler based on predefined test cases. For evaluation, Models are assessed on LiveCodeBench v5, comprising 880 problems that span from May 2023 to January 2025 (Jain et al., 2024), as well as HumanEval+ and MBPP+ (Liu et al., 2023). Since passing all unit tests is nearly impossible to achieve by guesswork, $\text{pass}@k$ provides a reliable measure of a model’s reasoning boundary.

The Effect of RLVR. As shown in Figure 4 and Figure 5 left, the effects of RLVR on three code generation benchmarks exhibit trends that are highly consistent with those observed in mathematical benchmarks. For instance, on LiveCodeBench, the original model achieves a $\text{pass}@1$ score of 23.8%, while the RLVR-trained model achieves 28.1%. However, when sampling 128 times, approximately 50% of coding problems can be solved by the original model, whereas only 42.8% are solved by the RLVR model. Furthermore, we observe that the slope of the original model’s curve remains steep at $k = 128$, suggesting that $\text{pass}@k$ will continue to increase with larger k values. In contrast, the curve for Code-R1 gradually converges. This suggests that while RLVR shows improvements in single-sample performance, it results in a diminishing coverage boundary and has less potential than the original model.

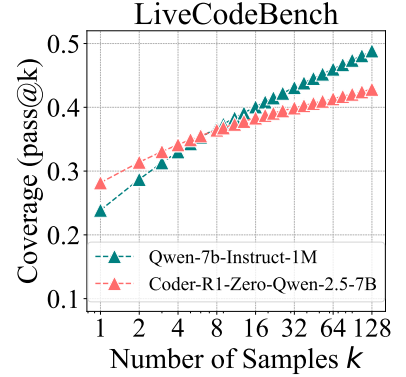


Figure 4: RLVR for Coding.

3.3. RLVR for Visual Reasoning

Models and Benchmarks. In visual reasoning, models must jointly interpret visual and textual inputs to solve complex reasoning problems. This has gained significant attention in the computer vision and multimodal communities since the rise of LLM reasoning (Chen et al., 2025; Shen et al., 2025; Zheng et al., 2025). For our experiments, we select mathematical reasoning within visual contexts as a representative task. We use the EasyR1 framework (Zheng et al., 2025) to train Qwen-2.5-VL-7B (Bai et al., 2025) on Geometry3K (Lu et al., 2021), and evaluate its visual reasoning capabilities on filtered MathVista-TestMini (Lu et al., 2024) and MathVision-TestMini (Wang et al., 2024). Specifically, both MathVista and MathVision contain multiple-choice questions, which can be easily guessed through repeated sampling. Therefore, we remove multiple-choice questions from the evaluation. After filtering, 460 problems remain out of 1000 in MathVista, and 114 problems remain out of 460 in MathVision.

The Effect of RLVR. As shown in Figure 5 (right), the effects of RLVR on visual reasoning are highly consistent with those observed in math and coding benchmarks. This suggests that the original model has broader coverage of solvable questions even in multimodal tasks.

Validity of Chain-of-Thought. To ensure that the increase in coverage is not due to random guessing with incorrect CoT, we manually inspect a subset of the most challenging problems, *i.e.* those with an average accuracy below 5%. For each inspected problem, we review all CoTs that led to correct answers. We find that for both the original and RL models, 7 out of 8 problems have *at least one* correct CoT. These results suggest that even on the hardest questions in the filtered set, the increase of coverage primarily results from sampling valid reasoning paths, rather than relying on lucky guesses.

4. Deep Analysis

In this section, we investigate the root cause of the phenomenon where RLVR improves sample efficiency but reduces the reasoning boundary. We also highlight the distinct properties of distillation compared to RLVR. In addition, we design controlled experiments to examine the effects of different RL algorithms.

4.1. Reasoning Patterns Already Present in Base Models

The RLVR Model’s Solvable-Problem Coverage is an Approximate Subset of the Base Model’s Coverage. Experiments in Section 3 surprisingly show that the base model has a larger

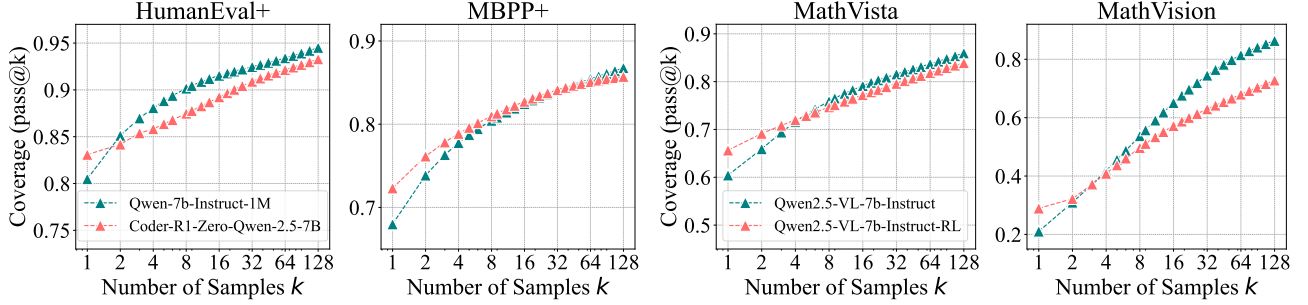


Figure 5: Pass@ k curves of base models and zero-RL counterparts. **(Left)** Code Generation. **(Right)** Visual Reasoning.

coverage of solvable problems than the RLVR-trained model. To further investigate, we compare the set of solvable questions for both the base model and its corresponding RL-trained version on AIME24. We find that the set of problems solved by the RL-trained model is nearly a subset of the solvable problems of the base model, as shown in Table 4. A similar trend is observed in coding tasks as shown in Table 5. This raises the natural question: Do all reasoning paths generated by RL-trained models already exist within the output distribution of their base models?

Perplexity Analysis. To answer this question, we utilize the metric *perplexity*. Given a model m , a problem x , and a response $\mathbf{Y} = (y_1, \dots, y_T)$ (can be generated by the same model, another model, or human), the perplexity is defined as the exponentiated average negative log-likelihood of a sequence:

$$\text{PPL}_m(\mathbf{Y}|x) = \exp \left(-\frac{1}{T} \sum_{t=1}^T \log P(y_t|x, y_1, \dots, y_{t-1}) \right),$$

which reflects the model’s ability to predict the given response \mathbf{Y} conditioned on the prompt x . Lower perplexity indicates that the model has a higher likelihood of generating this response.

We randomly sample two problems from AIME24 and employ Qwen-7B-Base and SimpleRL-Qwen-7B-Base to generate 16 responses for each problem, denoted as \mathbf{Y}_{base} and \mathbf{Y}_{RL} , respectively. We also let OpenAI-o1 (Jaech et al., 2024) generate 8 responses, denoted as \mathbf{Y}_{GT} . As shown in Figure 6 left, the distribution of $\text{PPL}_{\text{Base}}(\mathbf{Y}_{\text{RL}}|x)$ closely matches the lower portion of the $\text{PPL}_{\text{Base}}(\mathbf{Y}_{\text{Base}}|x)$ distribution, corresponding to responses that the base model tends to generate. This suggests that the responses from RL-trained models are highly likely to be generated by the base model. Combining the results from Section 3, we draw the following conclusions:

- **RLVR does not elicit novel reasoning abilities beyond the base model.** The trends of pass@ k at large values of k and the distribution of perplexity indicate that the reasoning coverage of the RL model remains entirely within that of the base model. All reasoning paths exploited by the RL model already exist within the base model. Thus, RL training does not introduce any fundamentally new reasoning capability, and the RL model remains bounded by the capabilities of its base model.
- **RLVR improves sampling efficiency.** Although the reasoning paths in the RL model already exist within the base model, RL training improves pass@1 performance, as shown in Section 3. This indicates that by biasing the output distribution toward high-reward responses, RL increases the likelihood of sampling correct reasoning paths that are already encoded in the base model.
- **RLVR narrows the reasoning boundary.** The efficiency gain of RLVR comes at the expense of coverage: pass@ k decreases at larger k values compared to the base model. We attribute this to the tendency of RL to reduce output entropy, which limits exploration (Yu et al., 2025).

4.2. Distillation Expands the Reasoning Boundary

In addition to direct RL training, another effective approach to improving the reasoning ability of small base models is distillation from a powerful reasoning model such as DeepSeek-R1 (Guo et al., 2025). This

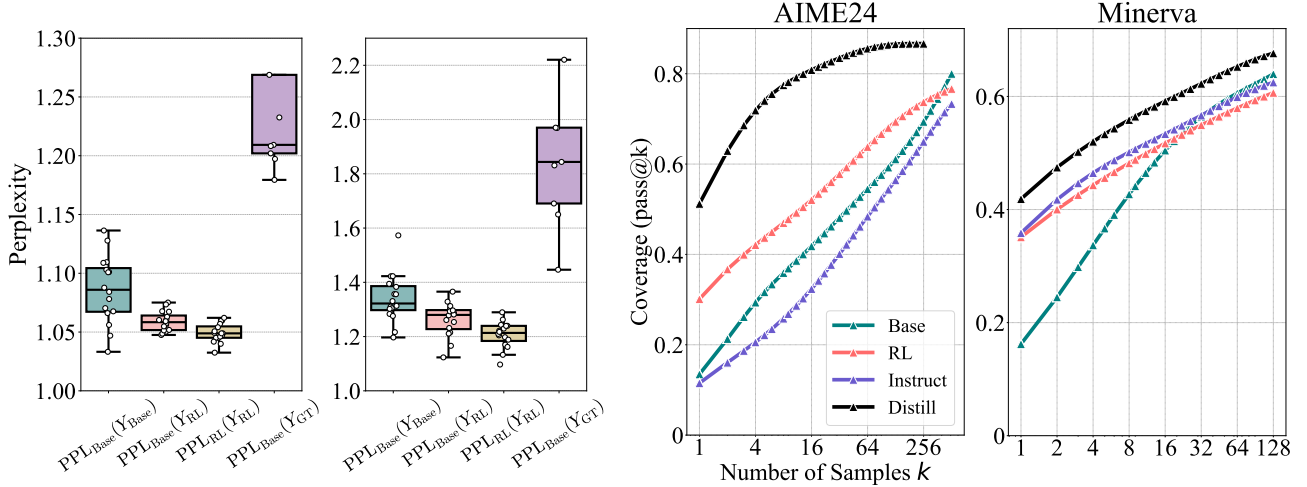


Figure 6: **(Left)** Perplexity distribution of responses from different sources, evaluated by the base and RL models. The conditioning problem x is omitted in the figure. **(Right)** Coverage comparison of base, Instruct, RL, and distilled models.

process is analogous to instruction-following fine-tuning in post-training, converting a base model into an instruct model. However, instead of using short instruction-response pairs, the training data consist of long CoT reasoning traces generated by DeepSeek-R1. Given the limitations of RLVR in expanding reasoning capabilities, it is natural to ask whether distillation exhibits similar behavior. We focus on a representative model, DeepSeek-R1-Distill-Qwen-7B, which distills DeepSeek-R1 into Qwen-2.5-Math-7B. We compare it with the base model Qwen-2.5-Math-7B and its RL-trained counterpart Qwen-2.5-Math-7B-Oat-Zero and include Qwen-2.5-Math-7B-Instruct as an additional baseline. As shown in Figure 6 (right), the pass@ k curve of the distilled model is consistently and significantly above that of the base model. This indicates that, unlike RL that is fundamentally bounded by the reasoning capacity of the base model, distillation introduces new reasoning patterns learned from a stronger teacher model. As a result, the distilled model is capable of surpassing the reasoning boundary of the base model.

4.3. Effects of Different RL Algorithms

As discussed previously, the primary effect of RL is to enhance sampling efficiency rather than to expand a model’s reasoning capacity. To quantify this, we propose the *Sampling Efficiency Gap* (Δ_{SE}), defined as the difference between the RL-trained model’s pass@1 and the base model’s pass@ k (we use $k = 256$ in our evaluation). Lower Δ_{SE} is better. Here we conduct clean experiments to study the effect of different RL algorithms in enhancing sampling efficiency.

Experiment Setup. We re-implement popular RL algorithms using the VeRL framework (Sheng et al., 2024) for fair comparison, including PPO (Schulman et al., 2017), GRPO (Shao et al., 2024), Reinforce++ (Hu, 2025), RLOO (Ahmadian et al., 2024), ReMax (Li et al., 2023), and DAPO (Yu et al., 2025). To assess in-domain and out-of-domain generalization under RLVR, we construct splits from Omni-MATH-Rule, a subset of Omni-MATH (Gao et al., 2024) containing verifiable problems. We split it into a training set (2,000 samples) and an in-domain test set (821 samples), and use MATH500 as the out-of-domain benchmark.

As shown in Figure 7 (top), although different RL algorithms exhibit slight variations in both pass@1 and pass@256, these differences are not fundamental. Different RL algorithms yield slightly different Δ_{SE} values (i.e., ranging from GRPO’s 43.9 to RLOO’s best 42.6 on the in-domain test set). Furthermore, we observe that Δ_{SE} remains consistently above 40 points across different algorithms, highlighting that existing RL methods are still far from achieving optimal sampling efficiency. This suggests that novel RL algorithms or entirely new paradigms may be necessary to approach the upper bound.

We also report several additional observations. First, DAPO achieves slightly higher pass@1 scores across all three datasets; however, its dynamic sampling strategy requires approximately $3 \sim 6\times$ more samples

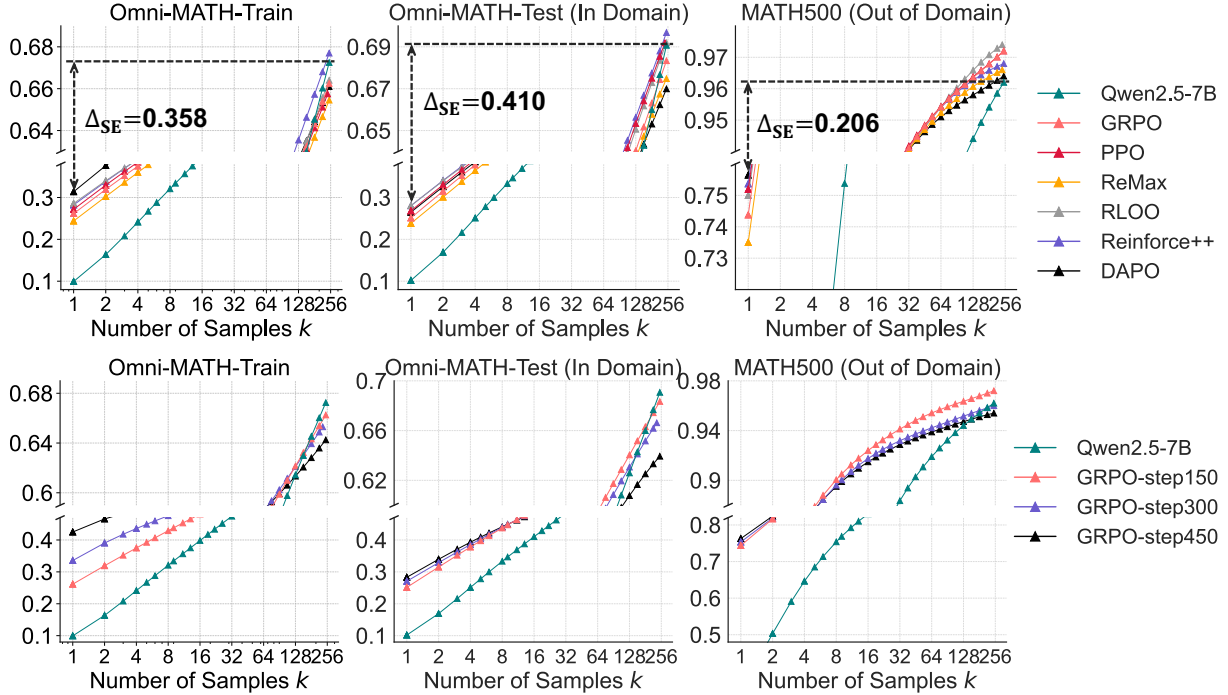


Figure 7: **(Top)** Different RL algorithms. **(Bottom)** Different RL training steps. We use a *folded y-axis* range to better highlight the details at $k = 1$ and 256. Unfolded version can be found in Figure 8. The detailed values for each point at $\text{pass}@1$ and $\text{pass}@256$ are provided in Table 2 and Table 3.

per batch during training compared to other algorithms. Moreover, its performance drops significantly at $k = 256$. Second, RLOO and Reinforce++ perform consistently well across the entire k range (from 1 to 256), while maintaining efficient training costs, achieving a good balance between effectiveness and efficiency. Third, ReMax shows lower performance at both $\text{pass}@1$ and $\text{pass}@256$. We hypothesize that this is due to its use of the greedy response reward as the advantage baseline, which in the RLVR setting is binary (0 or 1) and highly variable. This likely results in unstable gradient updates during training.

4.4. Asymptotic Effects of RL Training

Based on the setup in Section 4.3, we investigate the effect of the training steps on the asymptotic performance of the model. As shown in Figure 7 (bottom), as RL training progresses, $\text{pass}@1$ on the training set consistently improves from 26.1 to 42.5. However, several observations suggest that longer training may not yield substantial benefits. First, we observe that $\text{pass}@1$ after 450 steps on both in-domain and out-of-domain test sets shows only a marginal improvement compared to 150 steps, which is much smaller than the gain observed in the training set. This suggests that RL training might be overfitting the training set to some degree. Second, we find that as the number of training steps increases, $\text{pass}@256$ decreases across all three sets. Specifically, training for 450 steps results in the lowest $\text{pass}@256$, indicating a minimal reasoning boundary. This is likely because, as RL training progresses, the model’s output entropy and exploration ability decrease.

5. Discussion

In Section 3 and Section 4, we identified key limitations of RLVR in enhancing the LLM reasoning capabilities. In this section, we explore possible underlying factors that may explain why RLVR remains bounded by the reasoning capacity of the base model.

Discussion 1: Key Differences Between Traditional RL and RLVR for LLMs are Vast Action Space and Pretrained Priors. Traditional RL such as AlphaGo Zero and the DQN series (Silver

et al., 2017; Mnih et al., 2015; Yue et al., 2023) can continuously improve the performance of a policy in environments like Go and Atari games *without an explicit upper bound*. There are two key differences between traditional RL and RLVR for LLMs. First, the action space in language models is exponentially larger than that of Go or Atari games (Ramamurthy et al., 2023). RL algorithms were not originally designed to handle such a vast action space, which makes it nearly impossible to explore the reward signal effectively if training starts from scratch. Therefore, the second distinction is that RLVR for LLMs starts with a pretrained base model with useful prior, whereas traditional RL in Atari and GO games often begins from scratch. This pretrained prior guides the LLM in generating reasonable responses, making the exploration process significantly easier, and the policy can receive positive reward feedback.

Discussion 2: Priors as a Double-Edged Sword in This Vast Action Space. Since the sampling of responses is guided by the pretrained prior, the policy may struggle to explore new reasoning patterns beyond what the prior already provides. Specifically, in such a complex and highly combinatorial space, most responses generated during training are constrained by the base model’s prior. Any sample deviating from the prior is highly likely to produce invalid or non-sensical outputs, leading to negative reward. As discussed in Section 2.1, policy gradient algorithms aim to maximize the log-likelihood of responses within the prior that receive positive rewards, while minimizing the likelihood of responses outside the prior that receive negative rewards. As a result, the trained policy tends to produce responses already present in the prior, constraining its reasoning ability within the boundaries of the base model. From this perspective, training RL models from a distilled model may temporarily provide a beneficial solution, as distillation helps inject a better prior. In the future, exploration approaches that can explore beyond the confines of the prior in such a vast action space hold promise for creating more powerful reasoning models. Furthermore, alternative paradigms beyond pure RLVR could also be explored to overcome these limitations and enhance the model’s reasoning capabilities.

6. Related Works

Reinforcement Learning for LLM Reasoning. Since the emergence of LLMs, the post-training phase has proven crucial to enhance problem-solving and reasoning abilities (Ouyang et al., 2022). This stage typically falls into three main categories: supervised fine-tuning using human-curated or distilled data (Wang et al., 2023), self-improvement iteration (Zelikman et al., 2022; Gulcehre et al., 2023), and reinforcement learning (Ouyang et al., 2022). Previously, a reward model or preferences between responses were employed for reward modeling (Ouyang et al., 2022; Rafailov et al., 2023). Recently, Reinforcement Learning with Verifiable Rewards (RLVR) has gained significant traction as a method to improve the reasoning capabilities of LLMs in domains such as mathematics and programming (Lambert et al., 2024; Shao et al., 2024). An encouraging landmark work is OpenAI’s o1 model (Jaech et al., 2024), which was among the first large-scale applications of RL for reasoning, achieving state-of-the-art results at the time of its release. Following this, Deepseek-R1 (Guo et al., 2025) became the first open-weight model to match or surpass the performance of o1. A significant innovation introduced with R1 is the “zero” setting, where reinforcement learning is applied directly to the base LLM, bypassing any intermediate supervised tuning. This approach inspired a wave of open-source efforts to replicate or extend R1’s methodology and improve RL algorithms (Zeng et al., 2025; Liu et al., 2025b; Yu et al., 2025; Liu & Zhang, 2025). In parallel, reinforcement learning has also gained attention in the multimodal domain, driving advancements in multimodal reasoning (Chen et al., 2025; Shen et al., 2025; Zheng et al., 2025).

Although there are many excellent open-source works and algorithmic designs in the field of RLVR, there remains a lack of deep understanding regarding the root effects of RLVR on LLM reasoning abilities and its limitations when starting from the base model. Several studies (Liu et al., 2025a; Zhao et al., 2025; Shah et al., 2025) highlight that the reflective behaviors observed in R1-like models actually emerge from the base models, rather than being introduced by RLVR training. Dang et al. (2025) observed a phenomenon similar to our findings: Pass@k deteriorates rapidly and fails to recover with reinforcement learning, but this was seen only in a limited experimental setup with Qwen-2.5-0.5B on GSM8K. More importantly, they did not explore the relationship between the base model and the RL model. In contrast, our paper conducts systematic and rigorous experiments to show that not only reflective behaviors but

all reasoning paths are already embedded in the base model. We further demonstrate that RLVR does not elicit any new reasoning abilities beyond the base model.

7. Conclusion

RLVR is widely regarded as a promising approach to enable LLMs to continuously self-improve and acquire novel reasoning capabilities. In this paper, we systematically investigate the reasoning capability boundaries of both base and RLVR models across a wide range of LLM families and benchmarks, using the pass@ k metric coupled with manually checked CoTs. Surprisingly, our findings demonstrate that RLVR does not elicit fundamentally new reasoning patterns. Instead, RL primarily enhances the efficiency of LLMs in sampling existing correct reasoning paths encoded in the base model. Consequently, the reasoning boundary remains limited by the base model’s capabilities. Furthermore, our in-depth analysis reveals that current RL algorithms are far from achieving the optimal sampling efficiency, defined by the reasoning boundary of the base model. We also show that distillation plays a significant role in introducing new reasoning patterns and expanding the reasoning boundary. These findings highlight a critical limitation of RLVR in advancing LLM reasoning abilities, suggesting that a new paradigm may be necessary to fully surpass the capabilities of base models.

References

- Achiam, J., Adler, S., Agarwal, S., Ahmad, L., Akkaya, I., Aleman, F. L., Almeida, D., Altenschmidt, J., Altman, S., Anadkat, S., et al. Gpt-4 technical report. *arXiv preprint arXiv:2303.08774*, 2023. 1
- Ahmadian, A., Cremer, C., Gallé, M., Fadaee, M., Kreutzer, J., Pietquin, O., Üstün, A., and Hooker, S. Back to basics: Revisiting reinforce style optimization for learning from human feedback in llms. *arXiv preprint arXiv:2402.14740*, 2024. 5, 10
- Bai, S., Chen, K., Liu, X., Wang, J., Ge, W., Song, S., Dang, K., Wang, P., Wang, S., Tang, J., et al. Qwen2. 5-vl technical report. *arXiv preprint arXiv:2502.13923*, 2025. 8
- Brown, B., Juravsky, J., Ehrlich, R., Clark, R., Le, Q. V., Ré, C., and Mirhoseini, A. Large language monkeys: Scaling inference compute with repeated sampling. *arXiv preprint arXiv:2407.21787*, 2024. 2, 7
- Chen, L., Li, L., Zhao, H., Song, Y., and Vinci. R1-v: Reinforcing super generalization ability in vision-language models with less than \$3. <https://github.com/Deep-Agent/R1-V>, 2025. Accessed: 2025-02-02. 8, 12
- Chen, M., Tworek, J., Jun, H., Yuan, Q., Pinto, H. P. D. O., Kaplan, J., Edwards, H., Burda, Y., Joseph, N., Brockman, G., et al. Evaluating large language models trained on code. *arXiv preprint arXiv:2107.03374*, 2021. 5
- Cobbe, K., Kosaraju, V., Bavarian, M., Chen, M., Jun, H., Kaiser, L., Plappert, M., Tworek, J., Hilton, J., Nakano, R., Hesse, C., and Schulman, J. Training verifiers to solve math word problems. *arXiv preprint arXiv:2110.14168*, 2021. 6
- Dang, X., Baek, C., Kolter, J. Z., and Raghunathan, A. Assessing diversity collapse in reasoning. In *Scaling Self-Improving Foundation Models without Human Supervision*, 2025. URL <https://openreview.net/forum?id=AMiKsHLjQh>. 12
- Gao, B., Song, F., Yang, Z., Cai, Z., Miao, Y., Dong, Q., Li, L., Ma, C., Chen, L., Xu, R., Tang, Z., Wang, B., Zan, D., Quan, S., Zhang, G., Sha, L., Zhang, Y., Ren, X., Liu, T., and Chang, B. Omni-math: A universal olympiad level mathematic benchmark for large language models, 2024. URL <https://arxiv.org/abs/2410.07985>. 10
- Grattafiori, A., Dubey, A., Jauhri, A., Pandey, A., Kadian, A., Al-Dahle, A., Letman, A., Mathur, A., Schelten, A., Vaughan, A., et al. The llama 3 herd of models. *arXiv preprint arXiv:2407.21783*, 2024. 1, 6
- Gulcehre, C., Paine, T. L., Srinivasan, S., Konyushkova, K., Weerts, L., Sharma, A., Siddhant, A., Ahern, A., Wang, M., Gu, C., et al. Reinforced self-training (rest) for language modeling. *arXiv preprint arXiv:2308.08998*, 2023. 12
- Guo, D., Yang, D., Zhang, H., Song, J., Zhang, R., Xu, R., Zhu, Q., Ma, S., Wang, P., Bi, X., et al. Deepseek-r1: Incentivizing reasoning capability in llms via reinforcement learning. *arXiv preprint arXiv:2501.12948*, 2025. 1, 2, 3, 5, 9, 12
- He, C., Luo, R., Bai, Y., Hu, S., Thai, Z. L., Shen, J., Hu, J., Han, X., Huang, Y., Zhang, Y., et al. Olympiadbench: A challenging benchmark for promoting agi with olympiad-level bilingual multimodal scientific problems. *arXiv preprint arXiv:2402.14008*, 2024. 6
- Hendrycks, D., Burns, C., Kadavath, S., Arora, A., Basart, S., Tang, E., Song, D., and Steinhardt, J. Measuring mathematical problem solving with the math dataset. *NeurIPS*, 2021. 6
- Holtzman, A., Buys, J., Du, L., Forbes, M., and Choi, Y. The curious case of neural text degeneration. *arXiv preprint arXiv:1904.09751*, 2019. 2, 5

- Hu, J. Reinforce++: A simple and efficient approach for aligning large language models. *arXiv preprint arXiv:2501.03262*, 2025. 10
- Jaech, A., Kalai, A., Lerer, A., Richardson, A., El-Kishky, A., Low, A., Helyar, A., Madry, A., Beutel, A., Carney, A., et al. Openai o1 system card. *arXiv preprint arXiv:2412.16720*, 2024. 1, 9, 12
- Jain, N., Han, K., Gu, A., Li, W.-D., Yan, F., Zhang, T., Wang, S., Solar-Lezama, A., Sen, K., and Stoica, I. Livecodebench: Holistic and contamination free evaluation of large language models for code. *arXiv preprint*, 2024. 8
- Lambert, N., Morrison, J., Pyatkin, V., Huang, S., Ivison, H., Brahman, F., Miranda, L. J. V., Liu, A., Dziri, N., Lyu, S., et al. Tulu 3: Pushing frontiers in open language model post-training. *arXiv preprint arXiv:2411.15124*, 2024. 1, 12
- Lewkowycz, A., Andreassen, A., Dohan, D., Dyer, E., Michalewski, H., Ramasesh, V., Slone, A., Anil, C., Schlag, I., Gutman-Solo, T., et al. Solving quantitative reasoning problems with language models. *Advances in Neural Information Processing Systems*, 35:3843–3857, 2022. 6
- Li, Z., Xu, T., Zhang, Y., Lin, Z., Yu, Y., Sun, R., and Luo, Z.-Q. Remax: A simple, effective, and efficient reinforcement learning method for aligning large language models. *arXiv preprint arXiv:2310.10505*, 2023. 10
- Liu, A., Feng, B., Xue, B., Wang, B., Wu, B., Lu, C., Zhao, C., Deng, C., Zhang, C., Ruan, C., et al. Deepseek-v3 technical report. *arXiv preprint arXiv:2412.19437*, 2024. 6
- Liu, J. and Zhang, L. Code-r1: Reproducing r1 for code with reliable rewards. <https://github.com/ganler/code-r1>, 2025. GitHub repository. 7, 12
- Liu, J., Xia, C. S., Wang, Y., and Zhang, L. Is your code generated by chatGPT really correct? rigorous evaluation of large language models for code generation. In *Thirty-seventh Conference on Neural Information Processing Systems*, 2023. URL <https://openreview.net/forum?id=lqv610Cu7>. 8
- Liu, Z., Chen, C., Li, W., Pang, T., Du, C., and Lin, M. There may not be aha moment in r1-zero-like training — a pilot study. <https://oatllm.notion.site/oat-zero>, 2025a. Notion Blog. 12
- Liu, Z., Chen, C., Li, W., Qi, P., Pang, T., Du, C., Lee, W. S., and Lin, M. Understanding r1-zero-like training: A critical perspective. *arXiv preprint arXiv:2503.20783*, 2025b. 6, 12
- Lu, P., Gong, R., Jiang, S., Qiu, L., Huang, S., Liang, X., and Zhu, S.-C. Inter-gps: Interpretable geometry problem solving with formal language and symbolic reasoning. In *The 59th Annual Meeting of the Association for Computational Linguistics (ACL)*, 2021. 8
- Lu, P., Bansal, H., Xia, T., Liu, J., Li, C., Hajishirzi, H., Cheng, H., Chang, K.-W., Galley, M., and Gao, J. Mathvista: Evaluating mathematical reasoning of foundation models in visual contexts. In *International Conference on Learning Representations (ICLR)*, 2024. 8
- Mnih, V., Kavukcuoglu, K., Silver, D., Rusu, A. A., Veness, J., Bellemare, M. G., Graves, A., Riedmiller, M., Fidjeland, A. K., Ostrovski, G., et al. Human-level control through deep reinforcement learning. *nature*, 518(7540):529–533, 2015. 12
- Ouyang, L., Wu, J., Jiang, X., Almeida, D., Wainwright, C., Mishkin, P., Zhang, C., Agarwal, S., Slama, K., Ray, A., et al. Training language models to follow instructions with human feedback. *Advances in neural information processing systems*, 35:27730–27744, 2022. 12
- Rafailov, R., Sharma, A., Mitchell, E., Manning, C. D., Ermon, S., and Finn, C. Direct preference optimization: Your language model is secretly a reward model. *Advances in Neural Information Processing Systems*, 36:53728–53741, 2023. 12

- Ramamurthy, R., Ammanabrolu, P., Brantley, K., Hessel, J., Sifa, R., Bauckhage, C., Hajishirzi, H., and Choi, Y. Is reinforcement learning (not) for natural language processing: Benchmarks, baselines, and building blocks for natural language policy optimization. In *ICLR*, 2023. 12
- Schulman, J., Wolski, F., Dhariwal, P., Radford, A., and Klimov, O. Proximal policy optimization algorithms. *arXiv preprint arXiv:1707.06347*, 2017. 3, 10
- Shah, D. J., Rushton, P., Singla, S., Parmar, M., Smith, K., Vanjani, Y., Vaswani, A., Chaluvaraju, A., Hojel, A., Ma, A., et al. Rethinking reflection in pre-training. *arXiv preprint arXiv:2504.04022*, 2025. 12
- Shao, Z., Wang, P., Zhu, Q., Xu, R., Song, J., Bi, X., Zhang, H., Zhang, M., Li, Y., Wu, Y., et al. Deepseekmath: Pushing the limits of mathematical reasoning in open language models. *arXiv preprint arXiv:2402.03300*, 2024. 5, 10, 12
- Shen, H., Zhang, Z., Zhao, K., Zhang, Q., Xu, R., and Zhao, T. Vlm-r1: A stable and generalizable r1-style large vision-language model. <https://github.com/om-ai-lab/VLM-R1>, 2025. Accessed: 2025-02-15. 8, 12
- Sheng, G., Zhang, C., Ye, Z., Wu, X., Zhang, W., Zhang, R., Peng, Y., Lin, H., and Wu, C. Hybridflow: A flexible and efficient rlhf framework. *arXiv preprint arXiv: 2409.19256*, 2024. 10
- Silver, D., Schrittwieser, J., Simonyan, K., Antonoglou, I., Huang, A., Guez, A., Hubert, T., Baker, L., Lai, M., Bolton, A., et al. Mastering the game of go without human knowledge. *nature*, 550(7676): 354–359, 2017. 11
- Sutton, R. S., Barto, A. G., et al. *Reinforcement learning: An introduction*, volume 1. MIT press Cambridge, 1998. 5
- Team, K., Du, A., Gao, B., Xing, B., Jiang, C., Chen, C., Li, C., Xiao, C., Du, C., Liao, C., et al. Kimi k1. 5: Scaling reinforcement learning with llms. *arXiv preprint arXiv:2501.12599*, 2025. 1
- Wang, K., Pan, J., Shi, W., Lu, Z., Ren, H., Zhou, A., Zhan, M., and Li, H. Measuring multimodal mathematical reasoning with math-vision dataset. In *The Thirty-eight Conference on Neural Information Processing Systems Datasets and Benchmarks Track*, 2024. URL <https://openreview.net/forum?id=QWTCcxMpPA>. 8
- Wang, Y., Ivison, H., Dasigi, P., Hessel, J., Khot, T., Chandu, K., Wadden, D., MacMillan, K., Smith, N. A., Beltagy, I., et al. How far can camels go? exploring the state of instruction tuning on open resources. *Advances in Neural Information Processing Systems*, 36:74764–74786, 2023. 12
- Williams, R. J. Simple statistical gradient-following algorithms for connectionist reinforcement learning. *Machine learning*, 8:229–256, 1992. 5
- Yang, A., Yang, B., Zhang, B., Hui, B., Zheng, B., Yu, B., Li, C., Liu, D., Huang, F., Wei, H., et al. Qwen2. 5 technical report. *arXiv preprint arXiv:2412.15115*, 2024. 6
- Yang, A., Yu, B., Li, C., Liu, D., Huang, F., Huang, H., Jiang, J., Tu, J., Zhang, J., Zhou, J., et al. Qwen2. 5-1m technical report. *arXiv preprint arXiv:2501.15383*, 2025. 8
- Yu, Q., Zhang, Z., Zhu, R., Yuan, Y., Zuo, X., Yue, Y., Fan, T., Liu, G., Liu, L., Liu, X., et al. Dapo: An open-source llm reinforcement learning system at scale. *arXiv preprint arXiv:2503.14476*, 2025. 9, 10, 12
- Yue, Y., Kang, B., Xu, Z., Huang, G., and Yan, S. Value-consistent representation learning for data-efficient reinforcement learning. In *Proceedings of the AAAI Conference on Artificial Intelligence*, volume 37, pp. 11069–11077, 2023. 12
- Zelikman, E., Wu, Y., Mu, J., and Goodman, N. Star: Bootstrapping reasoning with reasoning. *Advances in Neural Information Processing Systems*, 35:15476–15488, 2022. 12

- Zeng, W., Huang, Y., Liu, Q., Liu, W., He, K., Ma, Z., and He, J. Simplerl-zoo: Investigating and taming zero reinforcement learning for open base models in the wild. *arXiv preprint arXiv:2503.18892*, 2025. 6, 12
- Zhao, R., Meterezh, A., Kakade, S., Pehlevan, C., Jelassi, S., and Malach, E. Echo chamber: Rl post-training amplifies behaviors learned in pretraining. *arXiv preprint arXiv:2504.07912*, 2025. 12
- Zheng, Y., Lu, J., Wang, S., Feng, Z., Kuang, D., and Xiong, Y. Easyrl: An efficient, scalable, multi-modality rl training framework. <https://github.com/hiyouga/EasyR1>, 2025. 8, 12

A. Detailed Experimental Results

The unfolded y-axis version of Figure 7 is provided in Figure 8, and the detailed values of pass@1 and pass@256 are given in Table 2 and Table 3. Indices of solvable problems in AIME24 and LiveCodeBench are provided in Table 4 and Table 5. Pass@ k curves in the filtered AIME24 are shown in Figure 9. The effects of different temperature settings are shown in Figure 10.

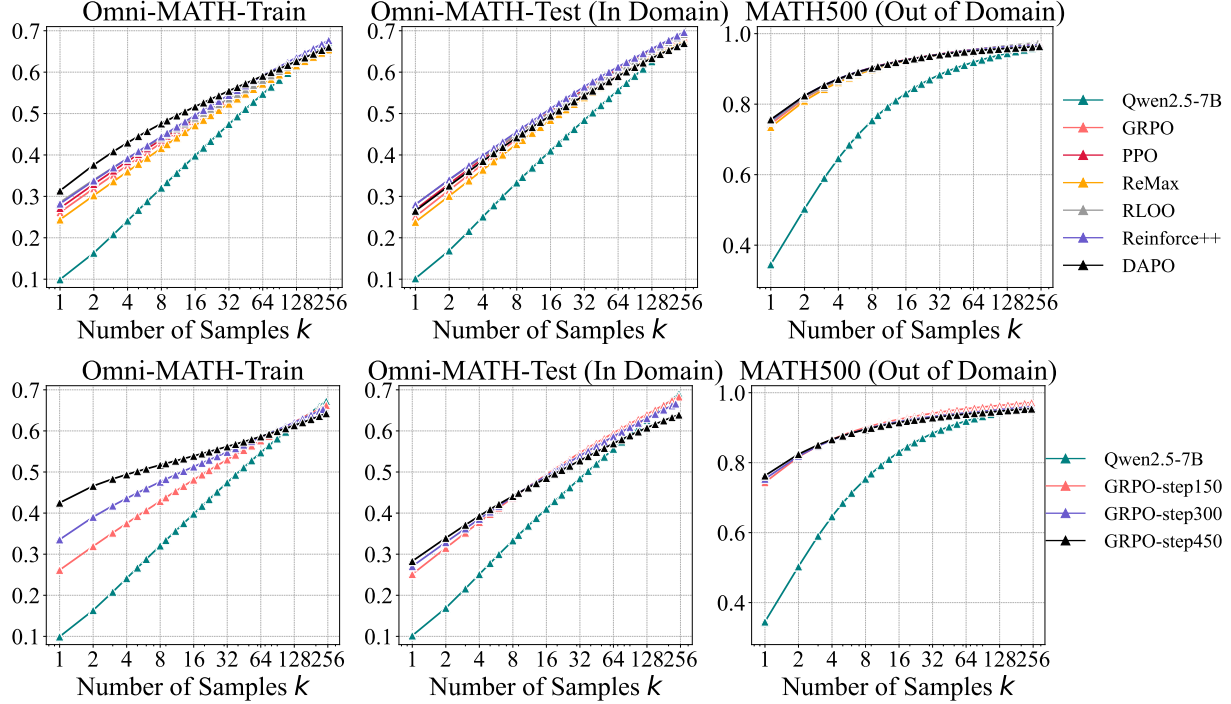


Figure 8: Unfolded y-axis version of Figure 7.

Table 2: Detailed values for each point at pass@1 and pass@256 across different RL algorithms in Figure 7.

Model	Omni-MATH-Train		Omni-MATH-Test		MATH500	
	pass@1	pass@256	pass@1	pass@256	pass@1	pass@256
Qwen2.5-7B	9.9	67.2	10.2	69.1	34.5	96.2
GRPO	26.1	66.3	25.1	68.3	74.4	97.2
PPO	27.2	65.8	26.8	69.2	75.2	97.2
ReMax	24.4	65.5	23.8	67.5	73.5	96.6
RLOO	28.6	66.4	28.1	69.2	75.0	97.4
Reinforce++	28.2	67.7	28.0	69.7	75.4	96.8
DAPO	31.4	66.1	26.5	67.0	75.6	96.4

Table 3: Detailed values at pass@1 and pass@256 across different RL training steps in Figure 7.

Model	Omni-MATH-Train		Omni-MATH-Test		MATH500	
	pass@1	pass@256	pass@1	pass@256	pass@1	pass@256
Qwen2.5-7B	9.9	67.2	10.2	69.1	34.5	96.2
GRPO-step150	26.1	66.3	25.1	68.3	74.4	97.2
GRPO-step300	33.6	65.3	27.1	66.6	75.4	96.0
GRPO-step450	42.5	64.3	28.3	63.9	76.3	95.4

Does Reinforcement Learning Really Incentivize Reasoning Capacity in LLMs Beyond the Base Model?

Table 4: Indices of solvable problems in AIME24 (starting from 0). An approximate subset relationship can be observed: most problems solved by the RL model are also solvable by the base model.

Models	Problem Indices
Qwen-7B-Base	0, 1, 4, 6, 7, 8, 9, 11, 12, 14, 15, 16, 17, 18, 19, 22, 23, 24, 25, 26, 27, 28, 29
SimpleRL-Qwen-7B	0, 1, 6, 7, 8, 9, 12, 14, 15, 16, 18, 22, 23, 24, 25, 26, 27, 28, 29

Table 5: Indices of solvable problems in LiveCodeBench (ranging from 400 to 450, starting from 0).

Model	Solvable Problem Indices
Qwen-7B-Instruct-1M	400, 402, 403, 407, 409, 412, 413, 417, 418, 419, 422, 423, 427, 432, 433, 436, 438, 439, 440, 444, 445, 448, 449
Coder-R1	400, 402, 403, 407, 412, 413, 417, 418, 419, 422, 423, 427, 430, 433, 438, 439, 440, 444, 445, 449

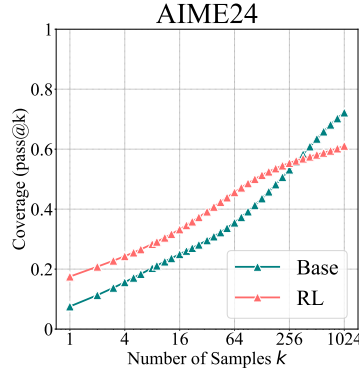


Figure 9: Pass@ k curves of the base and RL models in the filtered AIME24.

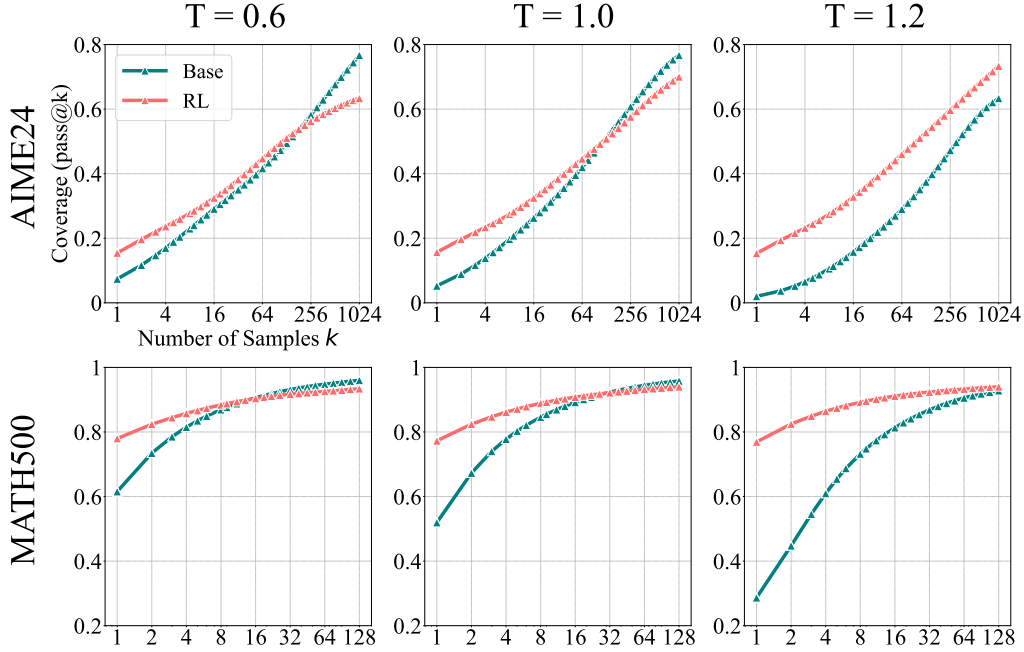


Figure 10: We found that the base model’s performance drops when the temperature exceeds 1.0, as it tends to generate more random and less coherent tokens. In contrast, the RL model’s performance remains relatively stable across different temperature settings. Therefore, we use $T = 0.6$ in the main experiments, as it allows both models to demonstrate their best reasoning performance.

B. Prompt Templates

We provide the prompt templates used for training and evaluation in our experiments. The prompt for SimpleRL training and evaluation is shown in Figure 11, while the prompt for Oat-Zero is shown in Figure 12. For Code-R1 training, prompt in Figure 13 is adopted. For Code-R1 evaluation, we follow the original codebase and adopt the default templates from the benchmarks, including LiveCodeBench prompt (Figure 14), HumanEval+, and MBPP+ prompt (Figure 15). The prompt used for EasyR1 training and evaluation is shown in Figure 16. For VeRL-trained RL models, as discussed in Section 4.3 and Section 4.4, the training and evaluation prompts are provided in Figure 17. To ensure a fair comparison, the base models use the same prompts as their corresponding RL-trained counterparts during evaluation.

C. Broader Impacts

The potential negative social impacts of our method align with those typically associated with general LLM reasoning technologies. We emphasize the importance of adhering to the principles of fair and safe deployment in LLM systems.

SimpleRL Prompt

```
<|im_start|>system
You are a helpful assistant.<|im_end|>
<|im_start|>user
{question}
Please reason step by step, and put your final answer within\\boxed{{ }}.<|im_end|>
<|im_start|>assistant
```

Figure 11: Prompt for SimpleRL Training and Evaluation. The base model uses the same prompt as the RL model during evaluation.

Oat Prompt

```
<|im_start|>system
Please reason step by step, and put your final answer within \\boxed{{ }}.<|im_end|>
<|im_start|>user
{question}<|im_end|>
<|im_start|>assistant
```

Figure 12: Prompt for Oat-Zero training and evaluation.

Code-R1 Prompt

```
<|im_start|>system
You are a helpful programming assistant. The user will ask you a question and you
as the assistant solve it. The assistant first thinks how to solve the task through
reasoning and then provides the user with the final answer. The reasoning process
and answer are enclosed within <think>...</think> and <answer>...</answer> tags,
respectively.<|im_end|>
<|im_start|>user
{question}<|im_end|>
<|im_start|>assistant
```

Figure 13: Prompt for Code-R1 training.

LiveCodeBench (Code Generation) Prompt

```
<|im_start|>system
You are a helpful assistant.<|im_end|>
<|im_start|>user
You will be given a question (problem specification) and will generate a correct
Python program that matches the specification and passes all tests. You will NOT
return anything except for the program.

Question: {question.question_content}

{ if question.starter_code }
### Format:
{PromptConstants.FORMATting_MESSAGE_WITH_STARTER_CODE}
```python
{question.starter_code}
```

<|im_end|>
{ else }
### Format:
{PromptConstants.FORMATting_MESSAGE_WITHOUT_STARTER_CODE}
```python
YOUR CODE HERE
```

<|im_end|>
<|im_start|>assistant
```

Figure 14: Prompt for Code-R1 Evaluation on LiveCodeBench.

HumanEval+ & MBPP+ Prompt

```
<|im_start|>system
You are a helpful assistant.<|im_end|>
<|im_start|>user
Please provide a self-contained Python script that solves the following problem in a
markdown code block:
```
{python_task_prompt}
```
<|im_end|>
<|im_start|>assistant
Below is a Python script with a self-contained function that solves the problem and
passes corresponding tests:
```python
```

Figure 15: Prompt for Code-R1 Evaluation on HumanEval+ and MBPP+.

#### EasyR1 Prompt

```
<|im_start|>system
You are Qwen, created by Alibaba Cloud. You are a helpful assistant. You FIRST
think about the reasoning process as an internal monologue and then provide the
final answer. The reasoning process MUST BE enclosed within <think> </think>
tags. The final answer MUST BE put in \boxed{ }.<|im_end|>
<|im_start|>user
<|vision_start|>{image_token}<|vision_end|>
{question}<|im_end|>
<|im_start|>assistant
```

Figure 16: Prompt for EasyR1 training and evaluation.

#### VeRL Training and Evaluation Prompt

```
<|im_start|>system
You are a helpful and harmless assistant. You are Qwen developed by Alibaba. You
should think step-by-step and put your final answer within \boxed{ }. <|im_end|>
<|im_start|>user
{question}<|im_end|>
<|im_start|>assistant
```

Figure 17: (1) Prompt for VeRL training and evaluation.

## Question

### (AIME24 Question No.16)

Among the 900 residents of Aimeville, there are 195 who own a diamond ring, 367 who own a set of golf clubs, and 562 who own a garden spade. In addition, each of the 900 residents owns a bag of candy hearts. There are 437 residents who own exactly two of these things, and 234 residents who own exactly three of these things. Find the number of residents of Aimeville who own all four of these things.

## Qwen-2.5-7B Answer

Response Length: 1058

To solve this problem, we can use the principle of inclusion-exclusion. We will denote the number of residents who own diamond rings, golf clubs, garden spades, and candy hearts as D, G, S, and C, respectively. We are given the following information:

- $D = 195$
- $G = 367$
- $S = 562$
- $C = 900$  (since every resident owns a bag of candy hearts)

We are also given that 437 residents own exactly two of these things and 234 residents own exactly three of these things.

Let's denote the number of residents who own all four of these things as X. We need to find X.

First, we need to find the number of residents who own at least one of these things. This can be calculated using the principle of inclusion-exclusion:

$$\begin{aligned} \text{Total} &= D + G + S + C - (\text{number of residents who own exactly two things}) \\ &\quad - 2 \times (\text{number of residents who own exactly three things}) - 3 \times (\text{number of residents who own all four things}) \end{aligned}$$

Since there are 900 residents in total, we can write the equation as:

$$900 = 195 + 367 + 562 + 900 - 437 - 2 \times 234 - 3 \times X$$

Now we need to solve for X:

$$\begin{aligned} 900 &= 195 + 367 + 562 + 900 - 437 - 468 - 3 \times X \\ 900 &= 1717 - 905 - 3 \times X \\ 900 &= 812 - 3 \times X \\ 3 \times X &= 812 - 900 \\ 3 \times X &= -88 \\ X &= -\frac{88}{3} \end{aligned}$$

**Since the number of residents cannot be negative, there is an error in our calculations. Let's re-evaluate the problem.**

We know that there are 437 residents who own exactly two things and 234 residents who own exactly three things. We can subtract these from the total number of residents who own at least one thing to find the number of residents who own exactly one thing:

$$\begin{aligned} \text{Number of residents who own exactly one thing} &= (D + G + S + C) - (\text{number of residents who own exactly two things}) \\ &\quad - 2 \times (\text{number of residents who own exactly three things}) - 3 \times (\text{number of residents who own all four things}) \end{aligned}$$

Let's denote the number of residents who own exactly one thing as Y:

$$\begin{aligned} Y &= (195 + 367 + 562 + 900) - 437 - 2 \times 234 - 3 \times X \\ Y &= 1924 - 905 - 3 \times X \\ Y &= 1019 - 3 \times X \end{aligned}$$

Since every resident owns at least one thing, we can write the equation:

$$900 = Y + 437 + 2 \times 234 + 3 \times X$$

Now we need to solve for X:

$$\begin{aligned} 900 &= (1019 - 3 \times X) + 437 + 468 + 3 \times X \\ 900 &= 1019 + 437 + 468 \\ 900 &= 1924 \end{aligned}$$

**This equation is not true, which means there is still an error in our calculations. Let's try a different approach.**

We can use the fact that the total number of residents who own at least one thing is 900. We can write the equation:

$$\begin{aligned} 900 &= (\text{number of residents who own exactly one thing}) + (\text{number of residents who own exactly two things}) \\ &\quad + (\text{number of residents who own exactly three things}) + (\text{number of residents who own all four things}) \end{aligned}$$

Let's denote the number of residents who own exactly one thing as Y:

$$\begin{aligned} 900 &= Y + 437 + 2 \times 234 + X \\ 900 &= Y + 805 + X \end{aligned}$$

Now we need to find Y. We can use the fact that the total number of residents who own at least one thing is equal to the sum of the residents who own each item minus the residents who own at least two items:

$$\begin{aligned} 900 &= (195 + 367 + 562 + 900) - (\text{number of residents who own exactly two things}) \\ &\quad - 2 \times (\text{number of residents who own exactly three things}) - 3 \times (\text{number of residents who own all four things}) \end{aligned}$$

$$\begin{aligned} 900 &= 1924 - 437 - 2 \times 234 - 3 \times X \\ 900 &= 1924 - 805 - 3 \times X \\ 900 &= 1119 - 3 \times X \end{aligned}$$

Now we can solve for X:

$$\begin{aligned} 3 \times X &= 1119 - 900 \\ 3 \times X &= 219 \\ X &= 73 \end{aligned}$$

So, the number of residents of Aimeville who own all four of these things is **73**.

Figure 18: Qwen-2.5-Base-7B Correct Response - Case 1.



## Question

## (AIME24 Question No.24)

Find the number of ways to place a digit in each cell of a  $2 \times 3$  grid so that the sum of the two numbers formed by reading left to right is 999, and the sum of the three numbers formed by reading top to bottom is 99. The grid below is an example of such an arrangement because  $8 + 991 = 999$  and  $9 + 9 + 81 = 99$ .

0	0	8
9	9	1

## Qwen-2.5-7B Answer

Response Length: 967

To solve this problem, we need to determine the number of ways to place digits in a  $2 \times 3$  grid such that the sum of the two numbers formed by reading left to right is 999, and the sum of the three numbers formed by reading top to bottom is 99. Let's break this down step by step.

## 1. Define the grid:

Let the grid be represented as:

$$\begin{array}{ccc} a & b & c \\ d & e & f \end{array}$$

The numbers formed by reading left to right are  $100a + 10b + c$  and  $100d + 10e + f$ . The numbers formed by reading top to bottom are  $10a + d$ ,  $10b + e$ , and  $10c + f$ .

## 2. Set up the equations:

- The sum of the two numbers formed by reading left to right is 999:

$$100a + 10b + c + 100d + 10e + f = 999$$

- The sum of the three numbers formed by reading top to bottom is 99:

$$10a + d + 10b + e + 10c + f = 99$$

## 3. Simplify the equations:

- From the first equation:

$$100a + 10b + c + 100d + 10e + f = 999$$

This implies:

$$a + d = 9, b + e = 9, c + f = 9$$

- From the second equation:

$$10a + d + 10b + e + 10c + f = 99$$

This is consistent with the previous simplification since:

$$10(a + b + c) + (d + e + f) = 99$$

Given  $a + d = 9$ ,  $b + e = 9$ , and  $c + f = 9$ , it follows that:

$$10(a + b + c) + (9 - a) + (9 - b) + (9 - c) = 99$$

Simplifying, we get:

$$10(a + b + c) + 27 - (a + b + c) = 99$$

$$9(a + b + c) + 27 = 99$$

$$9(a + b + c) = 72$$

$$a + b + c = 8$$

Since  $a + d = 9$ ,  $b + e = 9$ , and  $c + f = 9$ , and  $a + b + c = 8$ , it follows that:

$$d = 9 - a, e = 9 - b, f = 9 - c$$

## 4. Determine the possible values:

- $a, b, c$  must be digits (0-9) such that  $a + b + c = 8$ .
- For each valid combination of  $a, b, c$ ,  $d, e, f$  are uniquely determined as  $d = 9 - a$ ,  $e = 9 - b$ ,  $f = 9 - c$ .

## 5. Count the combinations:

- We need to count the number of non-negative integer solutions to  $a + b + c = 8$  with  $0 \leq a, b, c \leq 9$ .
- This is a classic "stars and bars" problem with an additional constraint. The number of solutions is given by the binomial coefficient:

$$\binom{8+3-1}{3-1} = \binom{10}{2} = 45$$

Therefore, the number of ways to place the digits in the grid is 45.

Figure 19: Qwen-2.5-Base-7B Correct Response - Case 2.